

## $k$ Spectrum of Passive Scalars in Lagrangian Chaotic Fluid Flows

Thomas M. Antonsen, Jr.,<sup>\*,†</sup> Zhencan Frank Fan,<sup>\*</sup> and Edward Ott<sup>\*,†,‡</sup>

University of Maryland, College Park, Maryland 20742

(Received 9 March 1995)

An eikonal-type description for the evolution of  $k$  spectra of passive scalars convected in a Lagrangian chaotic fluid flow is shown to accurately reproduce results from orders of magnitude more time consuming computations based on the full passive scalar partial differential equation. Furthermore, the validity of the reduced description, combined with concepts from chaotic dynamics, allows new theoretical results on passive scalar  $k$  spectra to be obtained. Illustrative applications are presented to long-time passive scalar decay, and to Batchelor's law  $k$  spectrum and its diffusive cutoff.

PACS numbers: 47.27.-i, 05.45.+b, 47.20.-k

The convection of a passive scalar by a fluid flow is a fundamental problem [1–10] that also has implications in a large number of practical contexts (e.g., chemical mixing, climate, etc.). The basic describing equation is the convection-diffusion equation,

$$\partial\phi/\partial t + \mathbf{v} \cdot \nabla\phi = D\nabla^2\phi + S, \quad (1)$$

where  $\phi(\mathbf{x}, t)$  is the passive scalar density,  $S(\mathbf{x}, t)$  is a source of the passive scalar,  $\mathbf{v}(\mathbf{x}, t)$  is the Eulerian fluid velocity (assumed incompressible  $\nabla \cdot \mathbf{v} = 0$ ), and  $D$  is the diffusion coefficient. Our interest is in situations in which  $D$  is small and  $\mathbf{v}(\mathbf{r}, t)$  varies on large spatial scale but induces Lagrangian chaos [1–9] in the sense that two nearby fluid elements convected by the flow diverge exponentially in time. In this case it has been shown that fine scale spatial variations in  $\phi$  are rapidly produced [1–6]. A particularly revealing characterization of such spatial structure is the wave-number power spectrum of  $\phi$ , which is often amenable to experimental measurement [7,8]. The wave-number power spectrum  $F(k, t)$  is defined by

$$F(k, t) = (2\pi)^{-n} \int d^n\mathbf{k}' \delta(k - |\mathbf{k}'|) \bar{C}(\mathbf{k}', t), \quad (2)$$

where  $n$  is the spatial dimensionality,  $\bar{C}(\mathbf{k}, t)$  is the spatial Fourier transform of the two point correlation function  $C(\mathbf{r}, t) = \langle \phi(\mathbf{x} + \mathbf{r})\phi(\mathbf{x}) \rangle$ , and the average indicated by the angle brackets is taken over the  $\mathbf{x}$  domain of Eq. (1).

While Eq. (1) appears simple, its numerical solution can be extremely demanding when  $D$  is small because of the large range of spatial scales produced. One goal of this Letter is to validate an eikonal-type set of ordinary differential equations for obtaining the power spectrum of passive scalars. We refer to these equations as the RKS description (reduced  $k$ -spectrum description). The RKS description will be shown to accurately reproduce results from orders of magnitude more time consuming computations based on the full partial differential equation [Eq. (1)]. Furthermore, the RKS description will also be shown to yield increased understanding, and this understanding, in conjunction with concepts from chaotic dynamics, will be used to obtain theoretical results.

In the rest of this Letter we will first introduce the RKS equations, and then apply them to two model

problems: (i) the long-time delay of a passive scalar, and (ii) Batchelor's law [7,10]  $k$  spectrum and its diffusive cutoff. The success obtained in these two cases suggests that the RKS description will be useful in other passive scalar problems as well.

*The reduced  $k$ -spectrum description.*—Consider a fluid element initially ( $t = 0$ ) located at position  $\mathbf{x}_0$ . Its position at a subsequent time  $t$  is denoted  $\mathbf{x}(\mathbf{x}_0, t)$ , where  $\mathbf{x}(\mathbf{x}_0, t)$  is the solution of

$$d\mathbf{x}/dt = \mathbf{v}(\mathbf{x}, t), \quad \mathbf{x}(\mathbf{x}_0, 0) = \mathbf{x}_0. \quad (3)$$

The flow is Lagrangian chaotic if initial differential displacements  $\delta\mathbf{x}_0$  typically yield exponentially growing displacements at subsequent time,  $|\delta\mathbf{x}|/|\delta\mathbf{x}_0| \sim \exp(ht)$ ,  $h > 0$ , where  $\delta\mathbf{x}$  satisfies

$$d\delta\mathbf{x}/dt = \delta\mathbf{x} \cdot \nabla\mathbf{v}(\mathbf{x}, t). \quad (4)$$

In the absence of diffusion and a source [ $D = 0$ ,  $S = 0$  in (1)], Eq. (1) implies that the scalar is constant following a fluid trajectory,  $d\phi/dt = 0$ . Thus the difference in  $\phi$  following two infinitesimally separated fluid elements is also constant  $d(\delta\mathbf{x} \cdot \nabla\phi)/dt = 0$ . Now imagine that we initially divide the fluid into many small areas. We consider the case in which the initial condition is in the form of a modulated sinusoidal function of  $\mathbf{x}$ ; that is,  $\phi(\mathbf{x}, 0) = A(\mathbf{x}) \sin[\int^{\mathbf{x}} \mathbf{k}(\mathbf{x}) d\mathbf{x} + \theta(\mathbf{x})]$  where  $\mathbf{k}$ ,  $A$ , and  $\theta$  vary on the scale of the flow that is much larger than  $|\mathbf{k}|^{-1}$ . We can then assign a mean wave vector to each area [11]. From  $d(\delta\mathbf{x} \cdot \nabla\phi)/dt = 0$  we have  $d(\delta\mathbf{x} \cdot \mathbf{k})/dt = 0$ . The evolution of each  $\mathbf{k}$  is then obtained by the use of (4),

$$d\mathbf{k}/dt = -(\nabla\mathbf{v}) \cdot \mathbf{k}. \quad (5)$$

Specializing to two-dimensional ( $x, y$ ) flows, the differential separation  $\delta\mathbf{x}$  in (4) will have two linearly independent solutions,  $\delta\mathbf{x}_1$  and  $\delta\mathbf{x}_2$ , which can be chosen so that  $|\delta\mathbf{x}_1|$  is exponentially increasing (chaos) while  $|\delta\mathbf{x}_2|$  is exponentially decreasing. The constancy of  $\delta\mathbf{x}_2 \cdot \mathbf{k}$  requires that  $\mathbf{k}$  be exponentially increasing in time except for the special case when  $\delta\mathbf{x}_2(0) \cdot \mathbf{k}(0) = 0$ . In this case, where  $\mathbf{k}(0)$  is perpendicular to the contracting direction of  $\delta\mathbf{x}$ , the constancy of  $\delta\mathbf{x}_1 \cdot \mathbf{k}$  along with the fact that

$\delta \mathbf{x}_2 \cdot \mathbf{k} = 0$  requires that  $\mathbf{k}$  be exponentially decreasing. Thus a typical choice of  $\mathbf{k}(0)$  eventually yields exponential growth,  $|\mathbf{k}(t)| \sim \exp(ht)$ . The initial conditions for which  $\delta \mathbf{x}_2 \cdot \mathbf{k} = 0$  (i.e.,  $\mathbf{k}$  is exponentially decreasing) represent a set of zero measure, yet, as we shall see, a small number of initial conditions close to these will dominate the long-time behavior of the scalar.

Under the present model, the spectrum is written as

$$F(k, t) = \sum_{\ell} \omega_{\ell}(t) \delta[k - |\mathbf{k}_{\ell}(t)|], \quad (6)$$

where  $\omega_{\ell}(t)$  is the variance contained in the  $\ell$ th initial area [ $\omega_{\ell}(t) = \int_{\ell} \phi^2 dx dy$ ], and  $\mathbf{k}_{\ell}(t)$  is the time evolving wave vector for the parcel of fluid in the  $\ell$ th area. In the absence of diffusion  $\omega_{\ell}(t)$  is constant in time. In the presence of diffusion, the total variance will decay at a rate determined by the diffusion coefficient and the local wave number,  $d\omega_{\ell}(t)/dt = -2k_{\ell}^2(t)D\omega_{\ell}(t)$ . Thus

$$\omega_{\ell}(t) = \omega_{\ell}(0) \exp\left[-2D \int_0^t k_{\ell}^2(t') dt'\right]. \quad (7)$$

Equations (3), (5), (6), and (7) constitute the RKS description [12,13]. The following numerical experiments show that these equations can provide a remarkably accurate approximation to the true solution.

*Long-time decay.*—We use a Fourier code [14] to solve Eq. (1) for  $\phi$  with  $S = 0$  and an initial condition,  $\phi(\mathbf{x}, 0) = 2\{\cos[2\pi(x - y)/L] - \cos[2\pi(x + y)/L]\}$ , with  $L$ -periodic boundary conditions in  $x$  and  $y$ . The flow  $\mathbf{v}$  is taken to be  $\mathbf{v}(\mathbf{x}, t)/v_0 = \{\mathbf{e}_x f_1(t) \cos[(2\pi y)/L] + \theta_1(t)\} + \{\mathbf{e}_y f_2(t) \cos[(2\pi x)/L] + \theta_2(t)\}$ . The functions  $f_1$  and  $f_2$  are periodic in time with period  $T$ ,  $f_1(t) = U[(T/2) - (t \bmod T)]$ ,  $f_2(t) = U[(t \bmod T) - (T/2)]$ , with  $U[\cdot]$  the unit step function.

The form of this flow is selected primarily because it is conveniently solved using the Fourier code. At any time only neighboring Fourier modes are coupled together, which allows for an efficient, implicit numerical solution of Eq. (1). The general conclusions we reach in the remainder of this Letter should not be dependent on this aspect of the flow.

If we set  $\theta_1 = \theta_2 = 0$ , then the flow is periodic in time, and, depending on  $\mathbf{x}_0$ , solutions of (3) yield either chaotic or nonchaotic [Kolmogorov-Arnold-Moser (KAM)] orbits. Here, to model a nonperiodic flow, we take the angles  $\theta_1$  and  $\theta_2$  to be different constant values randomly chosen in  $[0, 2\pi]$  for each period,  $MT \leq t < (M + 1)T$ . In this case there are no KAM surfaces. The solid curve in Fig. 1 shows the scalar variance  $C(t) = \int_0^L \int_0^L \phi^2 dx dy$  versus time obtained from the solution of (1) using the Fourier code. Here the parameters are  $v_0 T/L = 0.5$  and  $(2\pi/L)^2 DT = 1.25 \times 10^{-6}$ . Note the small value of the diffusion. We see from Fig. 1 that  $C(t)$  evidences a long-time exponential decay [4],  $C(t) \sim \exp(-\nu t)$  with  $\nu \cong 0.187$ . This damping rate

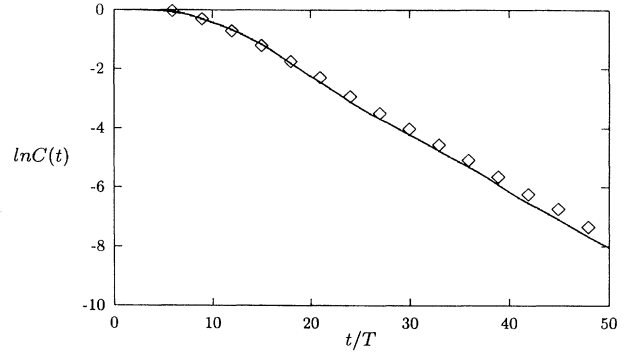


FIG. 1.  $\ln C(t)$  vs  $t/T$ ; the solid line represents the solution of Eq. (1) in Fourier space, and the diamonds are the results of the RKS model.

is found to be independent of  $D$  for small  $D$  [4]. The diamonds plotted in Fig. 1 show the results of repeating this calculation using the RKS description [15], where, by Parseval's theorem,  $C(t) = \sum \omega_{\ell}(t)$ . Clearly, the agreement is very good. Figure 2 shows results for the normalized  $k$  spectrum  $F_{\text{ave}}$  defined as  $F / \int F dk$  averaged over the times  $t/T = 21, 22, \dots, 30$ . The result from the Fourier code solution of (1) is plotted as dots, while the histogram plot obtained from the RKS equations is shown as a solid curve. These comparisons were made for slightly larger diffusion  $(2\pi/L)^2 DT = 5 \times 10^{-6}$ . Again good agreement is obtained.

*Batchelor's law and its diffusive cutoff.*—The above situation had no source of the passive scalar [ $S \equiv 0$  in Eq. (1)]. We now consider the case of a steady source at low wave number. In this case the time asymptotic wave number power spectrum  $F_s(k)$  is predicted to fall off with increasing wave number as  $k^{-1}$  [6,10] until a diffusive cutoff range is reached where the falloff is much faster than  $k^{-1}$ . This result is known as Batchelor's law. Figure 3 shows a plot of  $kF_s(k)$  vs  $k$  for the same flow as used for Figs. 1 and 2, but with a

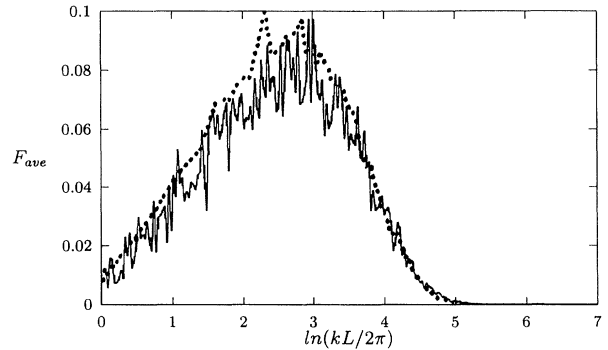


FIG. 2.  $F_{\text{ave}}$  vs  $kL/2\pi$ ; the dots correspond to the Fourier solution, and the solid curve corresponds to the RKS solution.

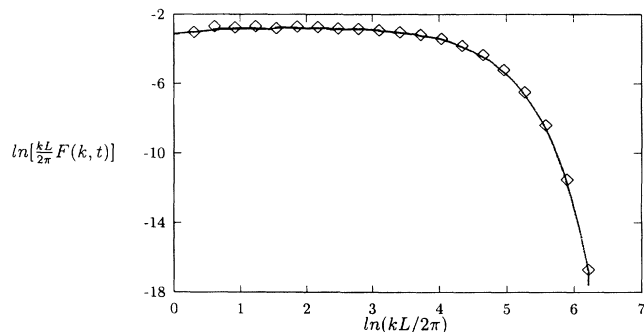


FIG. 3.  $(kL/2\pi)F_s(k)$  vs  $kL/2\pi$  for the case of a steady source of scalar variance. The solid line corresponds to the Fourier solution, and the diamonds correspond to the RKS solution.

steady source  $S = \cos(2\pi x/L + 2\pi y/L)$ . Batchelor's law dependence,  $kF_s(k) = \text{const}$ , is clearly seen in the region before the diffusive cutoff,  $k \lesssim (\nu_0/DL)^{1/2}$ . The results from the Fourier code (solid line) and the RKS equations (diamonds) [16] are almost identical.

**Analysis of long-time decay rate.**—The exponential decay of  $C(t) = \sum \omega_\ell(t)$  appearing in Fig. 1 can be evaluated by making use of (5) and (7). If one estimates the solution of (5) by  $k_\ell(t) \sim k_\ell(0)\exp(ht)$ , one finds that  $\omega_\ell$  is approximately constant until a time  $t_D \sim \ln[2h/k_\ell^2(0)D]/2h$  and then quickly decays to zero at a rate much faster than exponential. Thus most of the orbits do not contribute to the long-time decay of the exponential. To obtain the observed exponential decay we must consider exceptional initial wave vectors  $\mathbf{k}_\ell(0)$  that are nearly at right angles to the initial direction of exponential contraction of  $\delta\mathbf{x}$  [namely, at right angles to  $\delta\mathbf{x}_2(0)$ ]. In this case the estimate for the solution of (5) becomes  $k_\ell(t) \sim k_\ell(0)\cos\varphi_\ell\exp(ht)$ , where  $\varphi_\ell$  is the angle between  $\mathbf{k}_\ell(0)$  and the initial direction of exponential contraction of  $\delta\mathbf{x}$ . We then write  $C(t)$  as

$$C(t) = \int_0^\infty dh P(h, t) \times \int_0^{2\pi} \frac{d\varphi}{2\pi} \exp[-k_0^2 D h^{-1} \exp(2ht) \cos^2 \varphi], \quad (8)$$

where  $P(h, t)$  is the probability function of finite time Lyapunov exponents [17–20]. That is, if we choose an initial position in the flow at random and evaluate the largest Lyapunov exponent  $h$  for the orbit from that initial position over the time interval from time zero to time  $t$ , then  $P(h, t)dh$  is the probability that the exponent lies between  $h$  and  $h + dh$ . For large time, from theoretical considerations  $P(h, t)$  is well approximated by the scaling form [17–20]  $P(h, t) \equiv [tG''(h)/2\pi]^{1/2} \exp[-tG(h)]$  which expresses  $P(h, t)$  (which is a function of the two variables  $h$  and  $t$ ) in terms of a function of a single variable, namely, the function  $G(h)$ . This form has been nu-

merically verified and used for cases where there are no KAM surfaces (as in our examples). For large  $t$ , we can evaluate first the  $\varphi$  integral and then the  $h$  integral in (8) by noting the presence of saddle points at  $\varphi_s = \pi/2, 3\pi/2$  and at  $1 + G'(h_s) = 0$ . We obtain the exponential damping rate  $\nu$  [ $C(t) \sim \exp(-\nu t)$ ] as

$$\nu = h_s + G(h_s). \quad (9)$$

Note that  $\nu$  is independent of the diffusion coefficient  $D$ . To test the prediction (9), we have made histograms of  $P(h, t)$  from the orbits. From these we can evaluate  $G(h)$  via  $G(h) \equiv -t^{-1} \ln[P(h, t)/t^{1/2}]$ . Details appear in Ref. [14]. Using a polynomial fit by  $G(h)$ , Eq. (9) yields  $\nu = 0.191$  in agreement with the observed value of  $\nu \approx 0.187$ . Thus the long-time exponential decay is dominated by exceptional orbits whose initial  $\mathbf{k}_\ell(0)$  had only a small component in the direction of exponential growth of  $\mathbf{k}$  (contraction of  $\delta\mathbf{x}$ ).

Further, the dominant contribution comes from orbits with stretching rates  $h_s$  smaller than the mean  $\bar{h}$  where  $G'(\bar{h}) = 0$ . Thus this decay rate will be altered by the presence of KAM surfaces, which are excluded by the choice of the flow considered here but which are studied in Ref. [14].

In conclusion, we find that the RKS equations provide a remarkably accurate description of the evolution of passive scalar  $k$  spectra in Lagrangian chaotic fluid flows, and that they also provide useful analytical insight.

This work was supported by the Office of Naval Research.

\*Department of Electrical Engineering and Institute for Plasma Research.

†Department of Physics.

‡Institute for Systems Research.

- [1] H. Aref, *J. Fluid Mech.* **143**, 1 (1984).
- [2] J.M. Ottino, *The Kinematics of Mixing: Stretching, Chaos, and Transport* (Cambridge University Press, Cambridge, 1988).
- [3] J. Chaiken, C.K. Chu, M. Tabor, and Q.M. Tran, *Phys. Fluids* **30**, 687 (1987).
- [4] R. Pierrehumbert, *Chaos Solitons Fractals* **4**, 1091 (1994). This paper originally found that the long-time decay of scalar variance [ $C(t)$  in Fig. 1] is exponential and that the decay rate becomes independent of the diffusion coefficient  $D$  for small  $D$ .
- [5] E. Ott and T.M. Antonsen, *Phys. Rev. A* **39**, 3660 (1989); *Phys. Rev. Lett.* **61**, 2839 (1988).
- [6] T.M. Antonsen and E. Ott, *Phys. Rev. A* **44**, 851 (1991).
- [7] X.-I. Wu, B. Martin, H. Kellay, and W.I. Goldburg (to be published).
- [8] R. Ramashankar and J.P. Gollub, *Phys. Fluids A* **3**, 1344 (1991).
- [9] T.H. Solomon, E.R. Weeks, and H.L. Swinney, *Phys. Rev. Lett.* **71**, 3975 (1993).
- [10] G.K. Batchelor, *J. Fluid Mech.* **5**, 113 (1959).

- [11] More generally, if  $\phi(\mathbf{x}, 0)$  varies rapidly on the scale of the flow, we can assign a distribution of  $\mathbf{k}$ 's to each area. Approximating this distribution by discretization, Eq. (6) holds, where  $\omega_\ell(t)$  is the variance associated with each wave vector  $\mathbf{k}_\ell$ . A more rigorous derivation for this case will appear in a subsequent publication [14].
- [12] Equation (5) is the usual ray equation for  $\mathbf{k}$  obtained for the dispersion relation  $\omega = \mathbf{k} \cdot \mathbf{v}$  (corresponding to convection at velocity  $\mathbf{v}$ ) and was used in the eikonal formulations in Ref. [13]. In the case of no source or diffusion, the RKS description is simply a special case of the well-known Liouville equation for the conservation of the wave action density  $N(\mathbf{k}, \mathbf{x})$  in  $\mathbf{k}$ - $\mathbf{x}$  space,  $\partial N / \partial t + (\partial \omega / \partial \mathbf{k}) \cdot \partial N / \partial \mathbf{x} + (-\partial \omega / \partial \mathbf{x}) \cdot \partial N / \partial \mathbf{k} = 0$ .
- [13] S. Freidlander and M. Vishik, *Chaos* **1**, 198 (1991); A. Lifshitz and E. Hameiri, *Phys. Fluids A* **3**, 2644 (1991).
- [14] T. M. Anderson, Z. Fan, E. Ott, and E. Garcia-Lopez (to be published).
- [15] Since the initial condition involves two wave numbers,  $\mathbf{k} = (2\pi/L)(\mathbf{x}_0 \pm \mathbf{y}_0)$ , in our RKS computation we associate two wave numbers to each area and superpose their associated variances as mentioned in [11]. Note that, although the condition assumed to justify the RKS description (i.e.,  $|\mathbf{k}|^{-1} \ll L$ ) does not hold initially, the numerical results we obtain are still in agreement with the results from the Fourier code. In addition, if we are only interested in the damping *rate* of the variance, then this is independent of the detailed form of the initial condition.
- [16] The source is accommodated in the RKS calculation of  $F_s(k)$  (dots in Fig. 3) by superposing solutions of the initial value problem with initial value  $\phi(\mathbf{x}, t_n) = S(\mathbf{x})T$ , where  $t_n = nT$  denotes the initial times.
- [17] P. Grassberger, R. Badii, and A. Politi, *J. Stat. Phys.* **51**, 135 (1988).
- [18] H. Hata, T. Horita, H. Mori, T. Morita, and K. Tomita, *Prog. Theor. Phys.* **80**, 809 (1988).
- [19] E. Ott, C. Grebogi, and J. A. Yorke, *Phys. Lett. A* **135**, 343 (1989).
- [20] E. Ott, *Chaos in Dynamical Systems* (Cambridge University Press, Cambridge, 1993).